Photoelectrochemistry of n-Silicon and Bismuth(III) Iodide

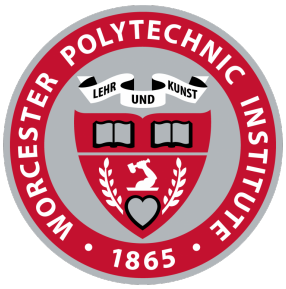

WPI

A Major Qualifying Project Report
Submitted to the Faculty of
WORCESTER POLYTECHNIC INSTITUTE
in partial fulfillment of the requirements for the
Degree of Bachelor of Science in Chemistry
By:

_____
Clare P. Masucci

Approved:

_____
Professor Ronald L. Grimm, Primary Advisor

Table of Contents

Table of Figures

Table of Tables

1. Abstract

We studied the open-circuit voltage of semiconductor electrodes in dual-liquid-junction photoelectrochemistry. One set of experiments utilized an acetylferrocene$^{+/0}$ redox couple as a back contact to n-Si(111) in a dual-liquid-junction solar cell, to further previous research in the Grimmgroup studying the effect of back-contact barrier heights on voltage in the n-Si cell. Separate experiments quantified the photoelectrochemical properties of bismuth(III) iodide, a compound of interest as a potential lead-free perovskite material for a perovskite/Si tandem solar cell without the toxicity of lead.

2. Introduction

2.1. Dual-liquid-junction photoelectrochemistry

N-type silicon is a well-researched material for photovoltaic cells.[i] Photoelectrochemical studies commonly employ a rectifying, liquid front contact, where electrons must overcome an energy barrier (barrier height) and an ohmic, or ideal, metal back contact, where the contact does not limit the current and voltage increases linearly.[ii,xi] Liquid-semiconductor junctions are useful because they can be used to study similar electrochemical properties but are nondestructive and allow for the silicon wafers to be cleaned and reused, and back and front contact combinations can be easily swapped. Having liquid junctions at both contacts, with the exception of cobaltocene$^{+/0}$, which forms an ohmic contact to n-Si, means that both junctions are rectifying, and there will therefore be two barrier heights for electrons to overcome. Previous work in the Grimmgroup hypothesized that a back-contact barrier height would negatively affect the open-circuit voltage of the cell according to eq 1 below.[xi]

$$V_{\mathrm{oc}} = \phi_{\mathrm{B,f}} - \boldsymbol{\phi_{B,b}} + \frac{kT}{q} \ln \frac{j_{\mathrm{ph}}}{AT^2} \qquad [1]$$

To test the effect of back-contact barrier heights in this model, the following redox couple combinations were used as back contacts to n-Si in a dual-liquid-junction cell with ferrocene$^{+/0}$ held constant as the front contact: ferrocene$^{+/0}$, cobaltocene$^{+/0}$, dimethylferrocene$^{+/0}$, octamethylferrocene$^{+/0}$, and decamethylferrocene$^{+/0}$. All of these redox couples have a barrier height less than or equal to that of ferrocene$^{+/0}$. The results (see Fig. 12) found that cobaltocene$^{+/0}$, which lacks a barrier height because its redox potential is greater than silicon's conduction band, had a large voltage (~450 mV).[xi] Redox couples with potentials between the Si band edges and with barrier heights less than or equal to ferrocene$^{+/0}$'s showed that back-contact barrier heights did negatively affect voltage, which decreased linearly as barrier heights increased, so the equation was determined to be valid.[xi] However, a redox couple, acetylferrocene$^{+/0}$, with barrier height greater than ferrocene$^{+/0}$'s, remained to be studied. One of the goals of this project was to complete the series of redox couples by synthesizing and testing acetylferrocene$^{+/0}$ as a back contact. Because the back-contact barrier height is greater than the front-contact barrier height in this setup, according to the equation we expect that the sign of the open-circuit voltage will flip and some samples will see a positive voltage.

2.2. Bismuth(III) iodide for solar energy applications

The properties of bismuth(III) iodide crystals have been studied since the early 1970s, with growth by vapor transport documented by 1995[iii]. Only more recently, since the 2000s, has the electronic properties of BiI_3 crystals and monolayers[iv] been studied particularly for the purposes of solar energy conversion[v,vi] and room temperature radiation detection[vii,viii,ix] due to its wide bandgap of ~1.7 to 1.8 eV[v,vi]. A bandgap this large is not ideal for a single-junction cell, but has potential for use in a tandem-junction cell with traditional silicon.[vi] Lead-containing perovskites are currently popular

materials for such tandem-junction cells, however, lead is toxic to humans and the environment. This makes lead-free BiI_3 more attractive, and it is accordingly gaining popularity in solar energy research, particularly in cells with BiI_3 thin films[vi] or monolayers.[iv] The performance of single-crystal BiI_3 has not yet, to the best of our knowledge, been studied in liquid-junction solar cells. This gap in knowledge is the motivation for applying our dual-liquid-junction cell model, previously used for n-Si, to BiI_3.

Since BiI_3 has a wider band gap than n-Si, its barrier height at the front contact to ferrocene$^{+/0}$ and our other redox couples is smaller. According the Equation 1 above, lower front contact-barrier heights lead to lower open-circuit voltage, while lower back contact-barrier heights lead to higher voltage. Because front-contact barrier heights are small for BiI_3, the selection of back contact materials with small barrier heights as well is key for building a cell with the highest open-circuit voltage possible. In the thin layer cell limited to the redox couples in Fig. 12, the combination of redox couple for highest V_{oc} is acetylferrocene$^{+/0}$ at the front and cobaltocene$^{+/0}$ at the back, similar to n-Si, if BiI_3 is n-type. In a liquid cell, however, BiI_3 electrodes can be created with traditional metal back contacts and a liquid front contact. This allows for studying metals like Au and Ag, with work functions ~5.4 eV and ~4.5 eV, respectively[x]. If BiI_3 behaves n-type, then the Ag metal contact would be expected to produce a cell with higher voltage, since its potential is higher than BiI_3's conduction band edge and would be an ohmic contact. The maximum open-circuit voltage for a BiI_3 with an ohmic back contact and maximum front-contact barrier height, calculated according to eq 1, is approximately 1.2 to 1.3 V.

3. Experimental

3.1. Synthesis and purification of redox couples

Ferrocene (98%, Aldrich) and acetylferrocene (97%, Alfa Aesar) were purified by sublimation. Acetylferrocenium tetrafluoroborate was synthesized by reaction of acetylferrocene with silver tetrafluoroborate (99%, Acros Organics) in diethyl ether, followed by filtration through PVDF syringe filters (13 mm, 0.10 μm, Advangene) and recrystallization in dichloromethane, all inside a glovebox under nitrogen. Solvents were degassed prior to use. The product was assessed by cyclic voltammetry in a three-electrode liquid cell with a platinum mesh counter electrode, platinum wire working electrode, and silver wire (0.5mm, ≥ 99.99%, Alfa Aesar) $Ag/AgNO_3$ reference electrode in a 20 mL solution of 50 mM acetylferrocene, 5mM acetylferrocenium tetrafluoroborate, and 1 M lithium perchlorate ($LiClO_4$) (battery grade, Sigma-Aldrich) in acetonitrile.

3.2. Thin layer n-Si cell setup

The dual-liquid-junction cell for testing n-Si was constructed according to Russell[xi] (Fig. 1): A copper wire was attached to 1 in. x 1 in. indium tin oxide (ITO) coated glass slides (8-12 Ω/sq., Aldrich) with GaIn alloy, covered with conductive silver paint (SPI Supplies), and reinforced with epoxy (Loctite 1C Hysol). Silicon samples ~ 1 cm x 2 cm were cleaned according to the RCA-1 and RCA-2 protocols and then treated with several drops of 2.45 M hydrofluoric acid (diluted from 49%, Transene) for 15 seconds on both sides to ensure the silicon was fully H-terminated. After the HF treatment, the samples were rinsed with water (18 MΩ, Millipore Milli-Q), dried with Argon, and promptly transferred to a nitrogen-filled glovebox until use.

Redox couple solutions were prepared from a premade solution of 1 M $LiClO_4$ in propylene carbonate (99.5% anhydrous, Acros Organics) and were stored over molecular sieves. Solutions were 100 mM in the metallocenes (5 mM for cobaltocene) and 5 mM in the metallocenium salts (100 mM for cobaltocenium).

For the electrochemistry experiments, the ITO slides were placed in a custom holder inside the glovebox with the wires connected to their respective potentiostat cables. Approximately 0.5 μL of the front redox couple solution was placed on the bottom slide, the silicon was placed on top, followed by 0.5 μL of the back redox couple solution. The top slide was placed on top and gently clamped down to form the thin film liquid layers.

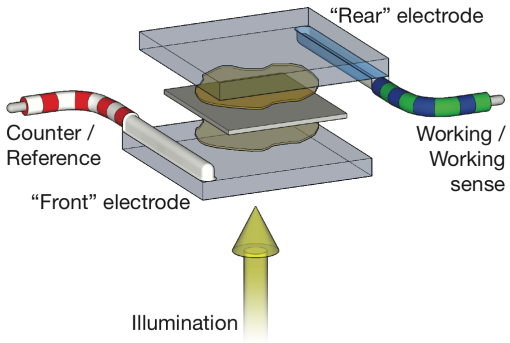

Figure 1. Dual-liquid-junction cell setup[xii]

*3.3. Bismuth(III) iodide synthesis**

BiI_3 was synthesized by chemical vapor transport. Stoichiometric amounts of bismuth and iodine (I_2) were vacuum-sealed in a glass or quartz tube prior to heating in a tube furnace for seven days at 390°C heating source side temperature and 370°C deposition side temperature. Tubes were opened and stored under nitrogen inside a glovebox and

shielded from light until use. Samples selected for electrochemistry experiments were flakes typically around 5 mm x 5 mm (Fig. 2).

Figure 2. BiI_3 sample used in the thin layer cell

*BiI_3 synthesis was conducted by Roy Stoflet.

3.4. Thin layer BiI_3 cell setup

Due to the thinness of the BiI_3 samples, a concern was that the cell could short if the back and front glass slides were to come into contact during an experiment. To prevent this, the slides were coated with an insulating PDMS plastic film. 1 in. x 1 in. pieces of fluorine-doped tin oxide (FTO) coated glass (~7 Ω/sq., Aldrich) were cleaned by successive 5 minute sonications in Alconox solution, isopropyl alcohol, and water. The cleaned slides were spin-coated with 3:1 PDMS (Sylgard 184) and toluene solution at 2000 rpm for one minute, and then the PDMS was cured by heating at 125°C for 20 minutes. After curing and cooling to room temperature, a section approximately 1 cm x 1 cm in the middle of the slide and a ~5 mm strip along one full side of the slide were cut with a razor blade and the PDMS was peeled off with tweezers. Testing resistance with a multimeter confirmed that conductivity was preserved after removing the PDMS layer and that the remaining PDMS was insulating as intended. A copper wire was attached to the PDMS-free strip on the side of the slide using GaIn alloy, silver paint, and epoxy (Loctite 9460 Hysol) as described in Section 3.2 above. Thin layer cells for photoelectrochemistry were constructed in the same manner as the n-Si cells, with the redox couples and BiI_3 placed between the slides inside the center PDMS-free sections. Smaller amounts (~0.2 μL) of redox couple solutions were used due to the small size of the BiI_3 flakes.

3.5. BiI_3 liquid cell setup

BiI_3 working electrodes were constructed by coating one side of the BiI_3 flakes with one of two back contact materials, connecting them to a copper wire housed in a glass tube with silver paint, and covering the connection with epoxy. Back contact materials were sputtered gold or the silver paint alone.

The electrodes were tested in a 20 mL of 1 M $LiClO_4$, 100 mM/5 mM ferrocene$^{+/0}$ and 5 mM/100 mM cobaltocene$^{+/0}$ solutions and stirred rapidly. A platinum wire electrode served as the reference electrode and a platinum mesh electrode served as the counter electrode. Both platinum electrodes were cleaned by washing in Alconox solution and rinsing with water prior to a 30 second dip in aqua regia (3:1 hydrochloric acid: nitric acid), followed by another rinse and dried with argon. Electrodes were left to further dry in an oven overnight at 100°C.

4. Results

4.1. Cyclic voltammetry of acetylferrocene$^{+/0}$

Cyclic voltammetry is a well-known technique for determining the potential of a redox couple. Current density is measured as potential is increased and then decreased for a known electrode in a redox couple solution. The forward scan, going up in potential, is anodic, meaning acetylferrocene is being oxidized to acetylferrocenium. The reverse scan is cathodic, and acetylferrocenium is reduced back to acetylferrocene. The peaks in current are used to calculate the half-wave potential, $E_{½}$, which approximates the formal potential of the redox couple and can be used to identify species in solution.

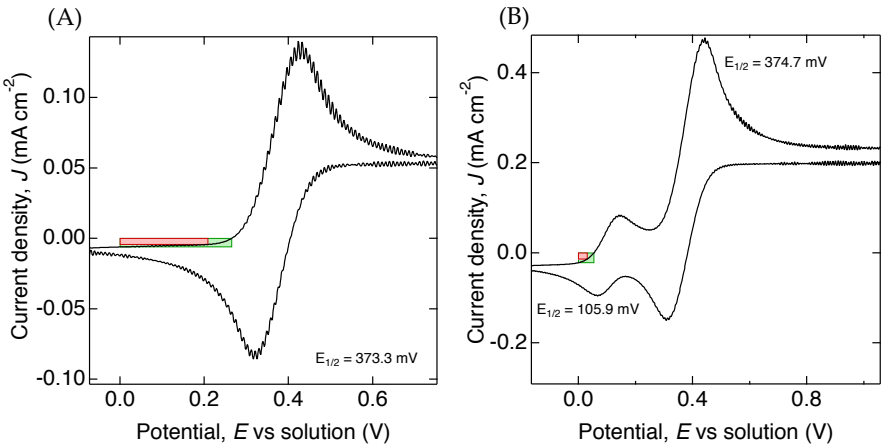

Figure 3. Cyclic voltammograms of acetylferrocene$^{+/0}$ in acetonitrile (A) and with ferrocene$^{+/0}$ added (B)

The current density v. potential scan (Fig. 3) displayed clear anodic and cathodic peaks on the forward and reverse scans, respectively. Over 5 scans, $< E_{½} > = 371.8 \pm 2.1$ mV vs. $Ag/AgNO_3$. After testing the acetylferrocene$^{+/0}$ redox couple, small amounts of ferrocene and ferrocenium hexafluorophosphate were added to the solution and the experiment was repeated. Ferrocene$^{+/0}$ has a less positive redox potential than acetylferrocene$^{+/0}$, and accordingly showed peaks at lower voltages. The difference in half-wave potentials of acetylferrocene$^{+/0}$ vs. ferrocene$^{+/0}$ was 269 mV, consistent with the literature value of 260 mV.[xii] These results, and the lack of extraneous wave features, indicate successful synthesis of acetylferrocenium tetrafluoroborate.

4.2. Thin layer n-Si cell

Current density v. potential scans of n-Si in the thin layer cell with acetylferrocene$^{+/0}$ as a back contact and ferrocene$^{+/0}$ as a front contact had both negative and positive open-circuit voltage in the light. Two representative scans are shown below in Fig. 4. For our calculations, samples with $V_{oc} < -150$ mV were discarded as outliers. Across the five remaining samples (in Table 1), V_{oc} ranged from –134.7 mV to 133.9 mV, with $<V_{oc}> = 13.7 \pm 115$ mV.

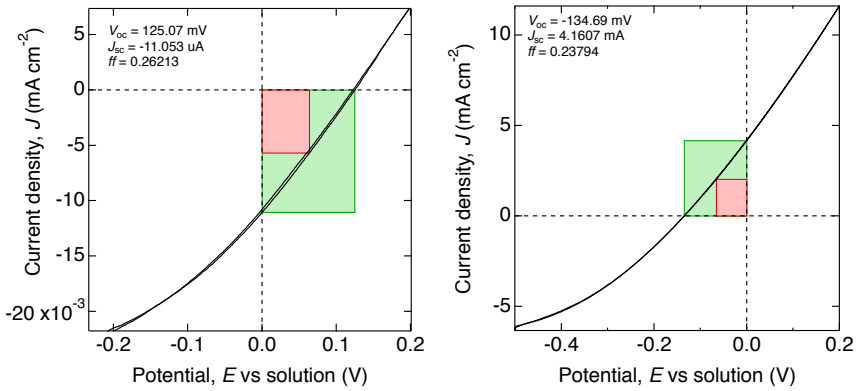

Figure 4. Current density v. potential of the thin layer n-Si cell with ferrocene$^{+/0}$ front, acetylferrocene$^{+/0}$ back

	Open-circuit voltage (V_{oc}) (mV)
Trial 1	– 6.41
Trial 2	133.9
Trial 3	125.07
Trial 4	– 49.6
Trial 5	– 134.7

Table 1. V_{oc} values for the thin layer n-Si cell with ferrocene$^{+/0}$ front, acetylferrocene$^{+/0}$ back

Cobaltocene$^{+/0}$ was also tested as a back contact and compared to expected and previously acquired data to confirm the cell was working properly. Because cobaltocene$^{+/0}$ and acetylferrocene$^{+/0}$ have the largest difference in redox potential, followed by cobaltocene$^{+/0}$ and ferrocene$^{+/0}$, open-circuit voltage is expected to be the largest for these combinations, close to the maximum V_{oc} of –600 mV. Results are shown in Table 2 below.

Front contact	Back contact	# of Samples	< V_{oc} > (mV)
Acetylferrocene$^{+/0}$	Cobaltocene$^{+/0}$	2	– 513
Ferrocene$^{+/0}$	Cobaltocene$^{+/0}$	2	– 494

Table 2. V_{oc} values for the thin layer n-Si cell with acetylferrocene$^{+/0}$ front, cobaltocene$^{+/0}$ back

4.3. Thin layer BiI_3 cell

With two different combinations of redox couples at the back and front contacts, BiI_3 thin layer cell experiments showed voltage responses when the light was turned on (between 2 - 4 seconds in Figs. 5 and 6). However, the direction of the response was not consistent between samples using the same combination of redox couples. Due to this inconsistency, $\langle V_{oc} \rangle$, and whether BiI_3 is n-type of p-type, could not be determined from this data. Further experiments will be needed for an accurate measurement of $\langle V_{oc} \rangle$.

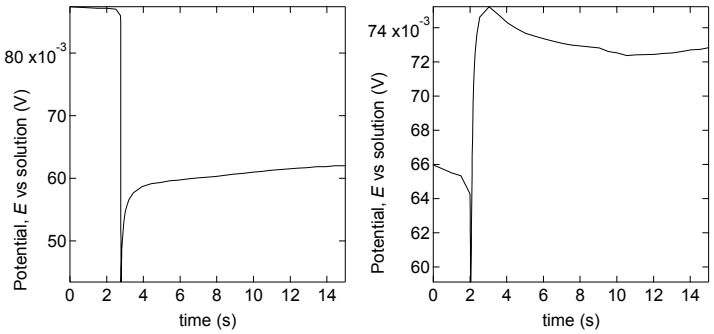

Figure 5. Potential v. time scans of the thin layer BiI_3 cell with ferrocene$^{+/0}$ front, acetylferrocene$^{+/0}$ back

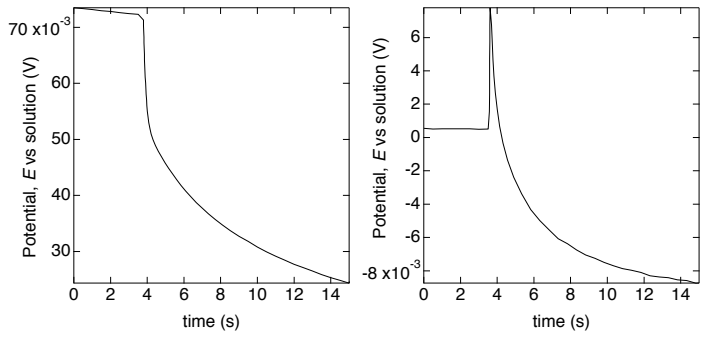

Figure 6. Potential v. time scans of the thin layer BiI_3 cell with acetylferrocene$^{+/0}$ front, cobaltocene$^{+/0}$ back

4.4. BiI_3 liquid cell

4.4.1. Liquid cell with ferrocene$^{+/0}$

In ferrocene$^{+/0}$, BiI_3 electrodes with both gold and silver as the back contact displayed similar results. V_{oc} was –56 mV and –45 mV, respectively, and both types of electrodes

had dark current close to zero, which is ideal for a solar cell. However, the voltages are far lower than the maximum of 1.2-1.3 V with Ag at the back. In Figs. 7 through 10, the dashed lines are scans taken in the absence of illumination, while solid lines were taken under ELH-simulated 1 sun illumination.

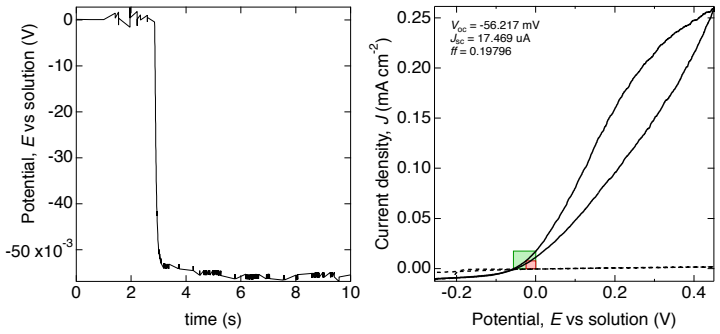

Figure 7. Potential v. time and current density v. potential of a Au-backed BiI_3 electrode in ferrocene$^{+/0}$

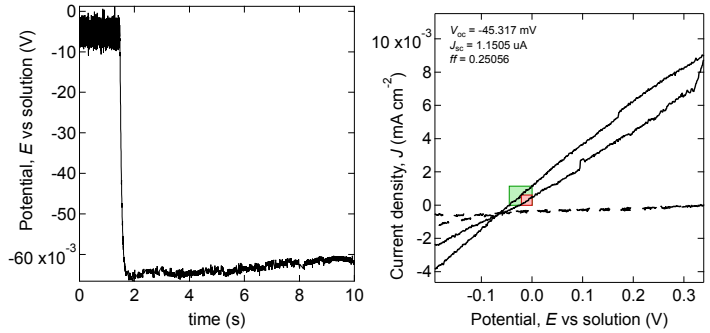

Figure 8. Potential v. time and current density v. potential of a Ag-backed BiI_3 electrode in ferrocene$^{+/0}$

4.4.2. Liquid cell with cobaltocene$^{+/0}$

Au-backed BiI_3 electrodes in cobaltocene$^{+/0}$ showed considerably worse performance than in ferrocene$^{+/0}$. Response to light was minimal, open-circuit voltage was effectively zero, and dark current exceeded light current over positive potentials.

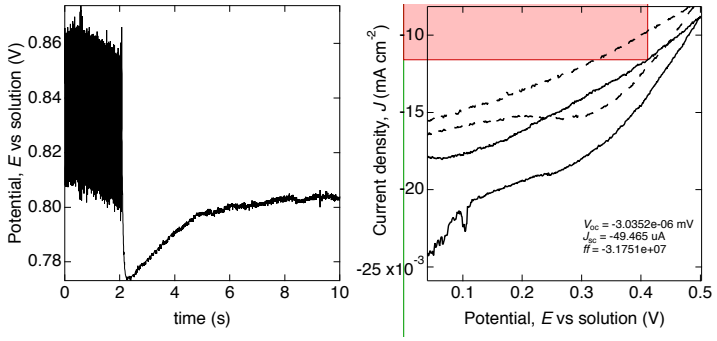

Figure 9. Potential v. time and current density v. potential of a Au-backed BiI_3 electrode in cobaltocene$^{+/0}$

Ag-backed electrodes also showed worse performance in cobaltocene$^{+/0}$. Again, response to light was minimal, open-circuit voltage was effectively zero, and dark current exceeded light current. The results for both back contacts indicate cobaltocene$^{+/0}$ is a poor front contact for bismuth iodide.

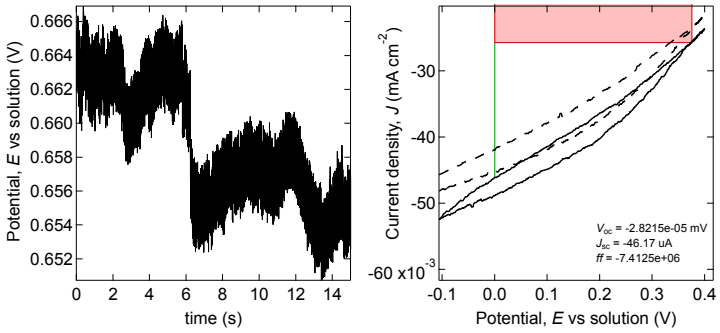

Figure 10. Potential v. time and current density v. potential of a Ag-backed BiI_3 electrode in cobaltocene$^{+/0}$

5. Discussion

Previous MQP work[x] derived Equation 1 (above in Section 2.1) to explain how barrier heights at the back contact can negatively impact cell voltage. Among the redox couples studied, the acetylferrocene$^{+/0}$ redox couple is unique as the only one with a back-contact barrier height greater than the ferrocene$^{+/0}$ front-contact barrier height (Fig. 11).

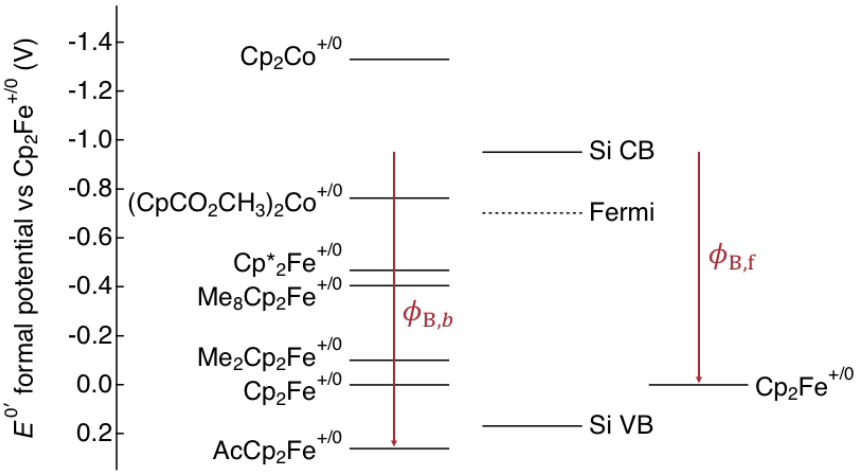

Figure 11. Band edges of silicon and various redox couples

The aforementioned prior work tested back contacts with $\phi_{B,b} < \phi_{B,f}$ and found that V_{oc} values agreed with the model. This research aimed to test if the model held when $\phi_{B,b} > \phi_{B,f}$, as is the case with acetylferrocene$^{+/0}$. The model predicts that open-circuit voltage values will reverse in sign from samples with the other redox couples as back contacts. A summary of results with the addition of the newly acquired data point for the ferrocene$^{+/0}$ front, acetylferrocene$^{+/0}$ back combination is shown in Fig. 12. Open-circuit voltages did change in sign across samples, supporting the model but leading to large error in $\langle V_{oc} \rangle$.

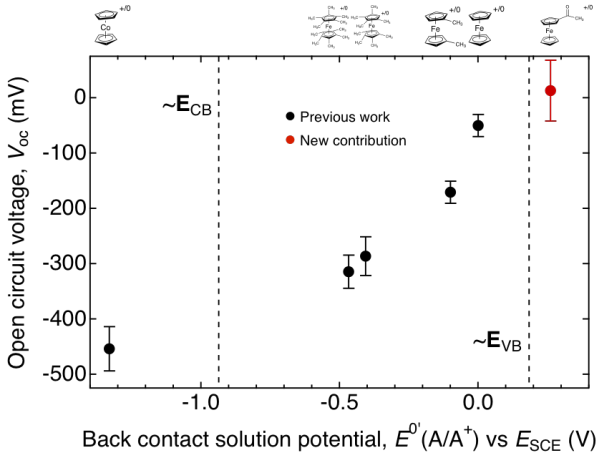

Figure 12. Experimental values for V_{oc} v. back contact solution potential in the n-Si thin layer cell

Results with cobaltocene$^{+/0}$ showed the highest voltage values seen in the n-Si thin layer cell for these experiments, with that of acetylferrocene$^{+/0}$ in the back greater than with ferrocene$^{+/0}$. This agrees with expectations and indicates the cell setup was functioning as desired.

The bismuth(III) iodide results were inconsistent and inconclusive overall. In the thin layer cell, the same combinations of redox couples produced voltage values of opposite sign between different samples of BiI_3. Unlike the ferrocene$^{+/0}$ front, acetylferrocene$^{+/0}$ back n-Si cell, sign flipping was not expected. Further experiments are needed before V_{oc} can be studied quantitatively, compared to the working model, and a diagram analogous to that in Fig. 12 can be produced for BiI_3. In the liquid cell, good light response and low dark current were seen for both Au and Ag back contact in ferrocene$^{+/0}$, but open-circuit voltage was very similar despite Au being a rectifying contact and Ag an ohmic contact, and far lower than the maximum potential for this cell.

6. Conclusions and Future Work

The open-circuit voltage values for the ferrocene$^{+/0}$ front, acetylferrocene$^{+/0}$ back redox couple combination in the n-Si cell behaved as expected according to Equation 1. This builds confidence in our model, leaving the future open to apply it to other materials of interest for solar cell applications, in order to study their photoelectrochemical properties. This was the motivation behind the bismuth(III) iodide experiments. However, results of the BiI_3 experiments in this project were inconclusive other than confirming a good response to light. Therefore, future work is needed to quantitatively determine the material's photoelectrochemical properties in our cell setups. The thickness of the BiI_3 samples and the PDMS layer on the FTO slides should be measured using SEM to ensure that the PDMS is an adequate thickness for preventing contact

between the FTO slides during experiments. Other future projects could include expanding the semiconductors used beyond n-Si and BiI_3.

7. References

[i] Kalan, R. E.; Russell, M. A.; Taylor, J. L.; Grimm, R. L. Dual Liquid Junction Photoelectrochemistry: Part I. Dual-Cuvette and Dual-Thin-Film Cells for Screening and Quantification of Back-Contact Properties. *J. Electrochem. Soc.* **2017**, *164* (12).

[ii] Kalan, R. E.; Russell, M. A.; Pugliese, A. J.; Carl, A. D.; Masucci, C. P.; Strandwitz, N. C.; Grimm, R. L. Dual Liquid Junction Photoelectrochemistry: Part II. Open-Circuit Photovoltage Variations Due to Surface Chemistry, Interfacial Dipoles, and non-Ohmic Junctions at Back Contacts. (in preparation; available upon request)

[iii] Nason, D.; Keller, L. The Growth and Crystallography of Bismuth Tri-Iodide Crystals Grown by Vapor Transport. *Journal of Crystal Growth* **1995**, *156* (3), 221–226.

[iv] Yan, H.; Ziyu, H.; Xu, G.; Xiaohong, S. Structural, Electronic and Photocatalytic Properties of Atomic Defective BiI 3 Monolayers. *Chemical Physics Letters* **2018**, *691*, 341–346.

[v] Sansom, H. C.; Whitehead, G. F. S.; Dyer, M. S.; Zanella, M.; Manning, T. D.; Pitcher, M. J.; Whittles, T. J.; Dhanak, V. R.; Alaria, J.; Claridge, J. B.; Rosseinsky, M. J. AgBiI4 As a Lead-Free Solar Absorber with Potential Application in Photovoltaics. *Chemistry of Materials* **2017**, *29* (4), 1538–1549.

[vi] Sasagawa, S.; Ebe, H.; Araki, H. Fabrication of Printable Thin Film Solar Cells Using BiI3 Absorption Layer. *Science of Advanced Materials* **2018**, *10* (5), 647–650.

[vii] Lintereur, A. T.; Qiu, W.; Nino, J. C.; Baciak, J. Characterization of Bismuth Tri-Iodide Single Crystals for Wide Band-Gap Semiconductor Radiation Detectors. *Nuclear Instruments and Methods in Physics Research Section A: Accelerators, Spectrometers, Detectors and Associated Equipment* **2011**, *652*(1), 166–169.

[viii] Matsumoto, M.; Hitomi, K.; Shoji, T.; Hiratate, Y. Bismuth Tri-Iodide Crystal for Nuclear Radiation Detectors. *IEEE Transactions on Nuclear Science* **2002**, *49*(5), 2517–2520.

[ix] Han, H.; Hong, M.; Gokhale, S. S.; Sinnott, S. B.; Jordan, K.; Baciak, J. E.; Nino, J. C. Defect Engineering of BiI3 Single Crystals: Enhanced Electrical and Radiation Performance for Room Temperature Gamma-Ray Detection. *The Journal of Physical Chemistry C* **2014**, *118* (6), 3244–3250.

[x] "Electron Work Function of the Crystalline Elements," in CRC Handbook of Chemistry and Physics, 98th Edition (Internet Version 2018), John R. Rumble, ed., CRC Press/Taylor & Francis, Boca Raton, FL.

[xi] Russell, M. A. Photoelectrochemical Voltage vs Back Contact Barrier Heights https://web.wpi.edu/Pubs/E-project/Available/E-project-042617-105441/.

[xii] Anari, E. H. B.; Romano, M.; Teh, W. X.; Black, J. J.; Jiang, E.; Chen, J.; To, T. Q.; Panchompoo, J.; Aldous, L. Substituted Ferrocenes and Iodine as Synergistic Thermoelectrochemical Heat Harvesting Redox Couples in Ionic Liquids. *Chemical Communications* **2016**, *52* (4), 745–748.